Available online at www.sciencedirect.com
SCIENCE DIRECT®
Polymer 44 (2003) 5597–5603
polymer
www.elsevier.com/locate/polymer

Synthesis, characterization and electrochemical properties of polybiselenophene

Teng-Teng Ong, Siu-Choon Ng*, Hardy S.O. Chan

Department of Chemistry, National University of Singapore, 3 Science Drive 3, Singapore, Singapore 117543

Received 3 June 2003; received in revised form 27 June 2003; accepted 30 June 2003

Abstract

A novel electrically conducting polymer consisting of selenophene moiety, poly(biselenophene) (PBSE) was generated by chemical and electrochemical polymerization. This polymer gave lower bandgap energy (1.9 eV) than pristine polyselenophene (2.0 eV). The electrochemical and optical properties of PBSE was investigated by UV–Vis near infrared spectroscopy and electrochemistry. In situ electrochemical doping studies of PBSE showed the formation of polaron states at 1.4 and 0.8 eV. Through cyclic voltammetry, the polymer oxidation potential (E_{pa}) and reduction potential (E_{pc}) for p-doping process for PBSE were observed at 0.93 and 0.86 V, respectively, at a scan rate of 20 mV s^{-1}. Upon chemical doping using chemical reagents such as iodine and ferric chloride, a maximum conductivity of 0.1 S cm^{-1} was achieved.

Keywords: Polybiselenophene; Electrochemistry; Conductivity

1. Introduction

The search for organic conducting polymers started in the 1970s, and since then many types of conducting polymers had been synthesized. The polymers that were reported largely focused on polyacetylene, polyaniline, polyfuran, polythiophene, polypyrrole and their functional derivatives, whilst relatively lesser work was conducted on polyselenophene [1–5]. Although the bandgap energy of polyselenophene has been reported to be the same as polythiophene (2.0 eV) [6] but, selenophene has lower oxidation potential and higher electron donating character than thiophene. [7] These showed that different composition of heteroatoms in similar systems can differ greatly in their electrical properties, chemical stability and ease of polymerization. Since polyselenophene has relatively large band gap in its neutral form, intensive research has been dedicated to chemical modifications of the polymer chemical structure with the aim to decrease the band gap [6]. Up to date, there are some literature reports on the pendant functionalized poly(3-methyl-selenophenes) [8], poly(3,4-ethylenedioxyselenophenes) [9] and poly(2,5-selenophene-diylvinylene) [10] (see Fig. 1). Among these polyselenophene derivatives being studied, polybiselenophene has not been reported. Accordingly, it will be interesting to conduct structure–property correlation studies on polybiselenophene. In this paper, we report the synthesis of biselenophene and its polymerization using both chemical and electrochemical methods. The obtained polybiselenophene is characterized and its properties will be compared with the pristine polyselenophene. In this way, we can analyze systematically and contrast the influence of the changes in polymer properties with structural modification. The electrochemical properties of polybiselenophene were analyzed using cyclic voltammetry (CV) whilst the optical properties of the polymer film were measured using UV–Vis near infrared spectroscopy. The properties of the bulk polymer was analysed by FTIR, elemental analysis and X-ray photoelectron spectroscopy (XPS).

* Corresponding author. Tel.: +65-68742675; fax: +65-67791691.
E-mail addresses: chmngsc@leonis.nus.edu.sg (S.C. Ng).

0032-3861/03/$ - see front matter © 2003 Elsevier Ltd. All rights reserved.
doi:10.1016/S0032-3861(03)00586-X

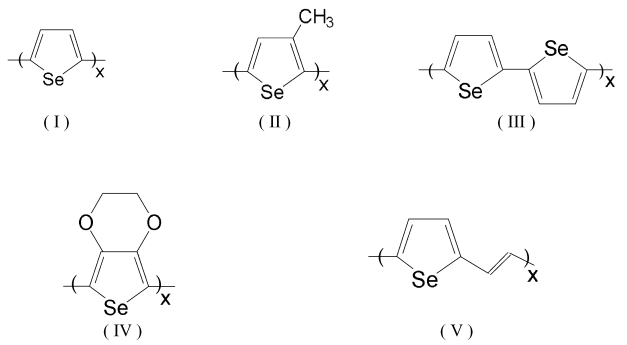

Fig. 1. Chemical structure of polymers, polyselenophene (I), poly(methyl-3-selenophene) (II), polybiselenophene (III), poly(3,4-ethylenedioxyseleno-phene) (IV), and poly(2,5-selenophendiyl-vinylene) (V).

2. Experimental

2.1. Materials

The following reagents were obtained from commercial sources, selenophene (Aldrich), bromine (BDH), *N*-bromosuccinimide (Merck), dichloro[1,3-bis(diphenylphosphino)-propane]nickel(II) (Fluka), ammonium chloride (Merck), anhydrous ferric chloride (Merck), calcium hydride (Fluka), nitromethane (Merck), tetra-n-butylammonium-tetrafluoroborate (Bu_4NBF_4)(TCI). The solvents used for synthesis were reagent grade solvents obtained from commercial sources, CS_2 (Merck), hexane (JT Baker), methanol (JT Baker), acetone (Merck), THF (JT Baker), ether (Merck) and chloroform (JT Baker).

2.2. Instrumentation

Elemental analysis of all compounds was performed using Perkin–Elmer 240C elemental analyser for C, H, N, and S determination. Infrared spectroscopy of monomers and polymers were performed by grinding sample with dry KBr powder and pressed under pressure to form circular KBr disks and recorded using a Perkin–Elmer 1600 spectrometer. ^{1}H NMR spectra were recorded on a Bruker ACF 300 FT-NMR spectrometer operating at 300 MHz, while ^{13}C NMR were recorded at 62.9 MHz. Mass spectra of organic compounds were obtained using a Micromass VG 7035E mass spectrometer at a source temperature of 200 °C. In situ electrochemical doping studies of polymers were carried out using and EG&G 263A potentiostat together with a Perkin Elmer Lamda UV–Vis near infrared spectrophotometer. Electrical conductivity measurements were carried out on polymer pellets of known thickness using a four-point probe connected to a Keithley constant current source system. Conductivity was calculated based on the average of at least ten pairs of consistent readings taken at different points of the pressed pellets. XPS analyses of polymers were performed using VG ESCA/SIMLAB MKII, with a Mg Kα radiation source (1253.6 eV). Surface elemental stiochiometries were obtained from peak area ratios corrected with the appropriate experimentally determined sensitivity factors.

2.3. Synthesis of 2-bromoselenophene

The synthesis of 2-bromoselenophene was performed according to methodology described in literature [11,12]. *N*-bromosuccinimide (13.3 g, 74.7 mol) was added in small amounts into selenophene (9.74 g, 74.4 mol) in 50 ml of dry chloroform at 0 °C. The reaction was stirred for 1 h at 0 °C. Extraction of organic phase with deionised water (2 × 100 ml) was carried out. The crude product was distilled under reduced pressure at 80 °C (30 mm Hg) to afford pure 2-bromoselenophene with yield of 56.8%. Mass spectra: (*m*/*e*) 209.9; ^{1}H NMR (300 MHz, $CDCl_3$, δ ppm) 7.01 (dd, β-1H, $J_{3-4} = 3.8$ Hz, $J_{2-3} = 6.1$ Hz), 7.22 (dd, β-1H, $J_{2-4} = 1.3$ Hz, $J_{3-4} = 3.9$ Hz), 7.88 (dd, α-1H, $J_{2-4} = 1.3$ Hz, $J_{2-3} = 6.1$ Hz); ^{13}C NMR (300 MHz, $CDCl_3$, δ ppm) 115.5, 129.8, 132.7, 132.8; microanalysis for C_4H_3BrSe (expected) C: 22.8%, H: 1.4%, Br: 38.1%, Se: 37.6%. (Found) C: 22.7%, H: 1.1%, Se: 38.0%, Br: 37.2% (weight reducing for Br analysis).

2.4. Synthesis of biselenophene

The synthesis of biselenophene was performed according to methodology described in literature [13,14]. Magnesium powder (0.17 g, 7.14 mmol) and a grain of iodine crystal was placed in a 10 ml round bottomed flask and filled with nitrogen. 2-bromoselenophene (1.58 g, 7.14 mmol) in 5 ml of dry THF was added dropwise to magnesium. After completion of addition, the reaction mixture was refluxed for 1.5 h. A second portion of 2-bromoselenophene (1.4 g, 6.67 mmol) in 3 ml of THF was added at 0 °C. Dichloro[1,3-bis(diphenylphosphino)propane]nickel(II) (0.02 g, 0.03 mmol) was added to catalyze the reaction. The reaction mixture was stirred for another 12 h before quenching with saturated ammonium chloride solution. The crude product was extracted with 20 ml of ether. The etheral layer was extracted twice using deionised water (2 × 30 ml). The combined ether extracts were concentrated to give a dark brown crude. Purification through flash chromatography with silica gel using hexane as eluent affords colourless crystalline solid with percentage yield of 40% and has a melting point of 67–68 °C. Mass spectra: (*m*/*e*) : 264; FTIR (KBr cell, cm^{-1}) 3110, 3062,1645, 1500, 1430, 1307, 1205, 1075, 1020, 819, 749, 683; ^{1}H NMR (300 MHz, $CDCl_3$, δ ppm) 7.20 (dd, β-2H, $J_{3-4} = 3.8$ Hz), 7.26 (dd, β-2H, $J_{2-4} = 2.4$ Hz), 7.88 (dd, α-2H, $J_{2-3} = 5.5$ Hz); ^{13}C NMR (300 MHz, $CDCl_3$, δ ppm) 129.7, 129.8 (β-4C), 131.0, 127.2 (α-4C); microanalysis for $Se_2C_8H_6$ (expected): C: 36.95%, H: 2.33%, Se: 60.73%. (Found): C: 36.88%, H: 2.21% and Se: 59.50%.

2.5. Chemical polymerization

Polybiselenophene was synthesized by reacting 1 mol equiv. of monomer with 4 mol equiv. of anhydrous ferric chloride in a 0.5 M monomer solution in dry chloroform. Polymerization was carried out for 1 h under nitrogen atmosphere at 0 °C. The as-synthesized polymer was greenish-black, suggestive of it being in the doped state. The polymer powder was filtered under suction and then subjected to Soxhlet extraction with methanol, followed by acetone for 24 h each.

2.6. Dedoping and doping of polymer

Dedoping of as-synthesized polymers was effected by stirring the polymer powder in a solution containing hydrazine hydrate and deionised water (v/v, 1: 1 ratio) for 24 h. After which, the polymer powder was filtered under suction and then subjected to Soxhlet extraction with methanol and acetone for 24 h each. The dedoped polymer powder was dried under high vacuum and appeared to be dark brown in colour.

Chemical redoping of the dedoped polymer was carried out by stirring the dedoped polymer powder in a solution containing 0.05 M ferric chloride dissolved in anhydrous nitromethane for 1 h under nitrogen atmosphere. The doped polymer powder was filtered under suction and rinsed with dry nitromethane. Iodine doping of dedoped polymer was conducted inside an iodine chamber where polymer pellets with known thickness and mass were placed inside the chamber over 24 h. The polymer pellets were taken out periodically and weighed to determine the iodine uptake, and their electrical conductivities were measured.

2.7. Electrochemical polymerization

Polymer thin films were directly grafted onto platinum foil and indium thin oxide (ITO) coated glass electrode using either CV, at which the potential was cycled between 0.0 and +1.2 V versus saturated calomel electrode (SCE) at 50 mV s^{-1}, or by galvanostatic method by applying a fixed current density of 0.5 mA cm^{-2}. Electrochemical polymerization was performed under argon atmosphere using a three-electrode single compartment electrochemical cell consisting platinum foil (0.5 cm^2) or ITO glass as the working electrode, a platinum wire as the counter electrode and $Ag/AgNO_3$ (0.1 M in dry acetonitrile) as the reference electrode which measured 0.34 V versus SCE. All experimental values in this report were corrected with respect to SCE. Standard monomer solutions (0.02–0.1 M) in 0.1 M supporting electrolyte Bu_4NBF_4 were used for electropolymerization.

2.8. Cyclic voltammetry

CV was conducted using monomer free electrolyte solution consisting of 0.1 M supporting electrolyte (Bu_4NBF_4) in acetonitrile. CVs of polymers were studied under argon atmosphere. For in situ UV–Vis near infrared-electrochemical doping studies, the polymer films were coated onto ITO glass and the quartz glass cells having path length of 1 cm was used instead of the standard electrochemical cells.

3. Results and discussions

3.1. Monomer synthesis

The reaction scheme for synthesis of biselenophene was depicted in Scheme 1. The synthesis of 2-bromoselenophene via direct bromination of selenophene using bromine was not feasible due to possible attack of halogens onto the ring heteroatom directly to generate selenienyl bromide.

An alternative method using *n*-bromosuccinimide yielded about 50% of pure 2-bromoselenophene [12]. Biselenophene was generated through Grignard coupling reaction of 2-bromoselenophene with 2-magnesiobromoselenophene using dry tetrahydrofuran as solvent [13,14]. The reaction mechanism involved the donation of electrons from the electron rich carbon–metal bond from Grignard reagent to the π-electron accepter in 2-bromoselenophene thus leading to the formation of symmetrical biselenophene. The use of $Ni(dppp)Cl_2$ catalyst is necessary in order to elevate the rate of reaction.

3.2. Polymerization and XPS measurements

The chemical oxidative polymerization of biselenophene afforded 90% yield. Both the dedoped and doped polybiselenophenes were insoluble in common organic solvents such as THF, DMF, and DMSO. Table 1 listed a comparison of the bulk and surface stoichiometries of the dedoped and doped polybiselenophene. The determined bulk stoichiometries of dedoped polybiselenophene (PBSE 1) correlated well to the expected values, while the ferric chloride doped (PBSE 2) polybiselenophene showed that significant amount of dopant had been incorporated into the bulk polymer. Surface stoichiometries obtained from XPS revealed a higher than expected carbon content for all three polymers PBSE 1, PBSE 2, and PBSE 3. The higher than expected carbon content is ascribable to surface hydrocarbon contamination commonly found in XPS studies.

The electrochemical polymerization of biselenophene

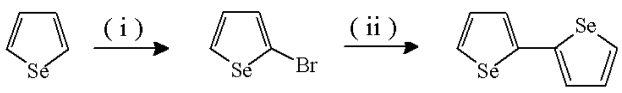

Scheme 1. Reaction scheme for synthesis of biselenophene and reaction conditions used (i) chloroform, *n*-bromosuccinimide, 0 °C; and (ii) Mg, I_2, dry THF, $Ni(dppp)Cl_2$, 0 °C, 2-bromoselenophene.

Table 1
Bulk and surface stoichiometries for dedoped polybiselenophene generated by chemical polymerization, PBSE 1, ferric chloride doped polymer, PBSE 2 and iodine doped polymer, PBSE 3

Polymer		Stoichiometries (bulk)	Stoichiometries (surface)
PBSE 1	[Expected] (Found)	$[Se_{2.0}H_{4.0}C_{8.0}Fe_{0.0}Cl_{0.0}]$ $(Se_{2.0}H_{5.4}C_{8.4}Fe_{0.0}Cl_{0.1})$	$[Se_{2.0}C_{8.0}Fe_{0.0}Cl_{0.0}]$ $(Se_{2.0}C_{8.4}Fe_{0.0}Cl_{0.1})$
PBSE 2	[Expected] (Found)	$[Se_{2.0}H_{4.0}C_{8.0}Fe_{>0.0}Cl_{>0.0}]$ $(Se_{2.0}H_{4.2}C_{8.6}Fe_{0.4}Cl_{0.1})$	$[Se_{2.0}C_{8.0}Fe_{>0.0}Cl_{>0.0}]$ $(Se_{2.0}C_{8.4}Fe_{0.0}Cl_{0.1})$
PBSE 3	[Expected] (Found)	$[Se_{2.0}H_{4.0}C_{8.0}Fe_{>0.0}Cl_{>0.0}]$ $(Se_{2.0}H_{4.3}C_{8.5}Fe_{0.0}Cl_{0.1})$	$[Se_{2.0}C_{8.0}Fe_{>0.0}Cl_{>0.0}]$ $(Se_{2.0}C_{8.4}Fe_{0.0}Cl_{0.1})$

can be effected using either potentiostatic or galvanostatic methods, as well as CV. The polymerization of biselenophene by galvanostatic method was being shown in Fig. 2(a), using 0.05 M in Bu_4NBF_4 electrolyte in acetonitrile at 25 °C, with a fixed current density of 0.5 mA cm^{-2}. The monomer oxidation potential for biselenophene was being deduced to be 1.15 V versus SCE. The doped polymer film was greenish-blue in colour. Upon dedoping, it turned reddish brown in colour.

In Fig. 2(b), the electrochemcial polymerization of biselenophene using CV technique was being shown. Electrochemical polymerization was initiated by setting the potentiostat to cycle from 0.0 to 1.2 V repeatedly. During the first scan, no apparent redox peaks were observed during the first scan. As the number of scans increases, the cathodic peak at 0.8 V increases in intensity. An anodic peak at approximately 0.9 V, corresponding to the oxidation of PBSE was observed. As the polymerization proceeds, the peak current increases with successive scans, indicating the growth of polymer onto the surface of the electrode. During the 20th CV scan, two peaks corresponding to E_{pa} at 1.0 V and E_{pc} at 0.8 V versus SCE were being observed. The obtained polybiselenophene, PBSE film appeared reddish brown in their neutral state and greenish-blue when electrochemically doped.

3.3. Electrochemistry of polybiselenophene

The electrochemistry of polybiselenophene (PBSE), was studied in monomer free solution. During the p-doping process, the polymer film deposited on platinum electrode was cycled repeatedly between the conducting (oxidised) and non-conducting (neutral) state without showing significant decomposition of the polymer film. The cyclic voltammogram of PBSE showing the p-doping at different scan rates was displayed in Fig. 3. The polymer oxidation potential (E_{pa}) and reduction potential (E_{pc}) for p-doping process for PBSE was observed at 0.93 and 0.86 V, respectively, at a scan rate of 20 mV s^{-1}. From CV data reported by Waltman et al. [19], the polymer oxidation potential for polybithiophene was 1.0 V, which was comparable to polybiselenophene (0.93 V).

During the p-doping process of PBDE, strong electrochromism was observed, showing contrasting colour changes from reddish-brown when in its dedoped form to dark green when in its doped form. The ratio of E_{pa}/E_{pc} was determined to be about 1.1, indicating that the doping/undoping process is generally reversible in nature. The coulombic charges for both the oxidation (Q_o) and reduction (Qr) processes during the CV scan for PBSE were calculated from the CV plot. The electrochemical data on changes in peak currents amd redox potentials of PBSE during p-doing at different scan rates and the integrated charge for the anodic current for p-doping was shown in Table 2. For PBSE, the coulombic recovery (Q_r/Q_o), for p-doping process was ranged between 58 and 86%. The n-doping process of PBSE was found to be unstable, no accompanied anodic and reduction peak were detected when the potential was cycled to extreme negative potentials up to −2.4 V versus SCE.

3.4. Optical analysis of polybiselenophene

Polymer thin films which were grafted onto conducting ITO glass electrode were first subjected to electrochemical dedoping by subjecting the polymer film to a voltage from +1.0 to −0.3 V versus SCE to ensure that the polymer films were in their neutral state. The UV–Vis absorption spectrum of dedoped PBSE film in ITO glass exhibits an absorption maximum (λ_{max}) at 498 nm. A red shift in λ_{max} with respect to polyselenophene (440 nm) [15], was observed for polybiselenophene. In polythiophene–polybithiophene system [17–20], a similar phenomenon was observed. The observed λ_{max} for polybithiophene (475 nm) [18] showed a red shift compared to polythiophene (450 nm) [17].

The band gap energy of PBSE may be derived from the

Table 2
Electrochemical data on changes in peak currents and redox potentials of PBSE during p-doing at different scan rates and the integrated charge for the anodic current for p-doping. CV data for p-doping process was obtained using 0.1 M tetra-*n*-butylammonium-tetrafluoroborate in dry acetonitrile under argon atmosphere at room temperature

Scan rate (mV s^{-1})	E_{pa} (V)	E_{pc} (V)	I_{pa} (mA)	I_{pc} (mA)	Q_o (mC)	Q_r (mC)	Q_r/Q_o (%)
20	0.896	0.769	0.014	−0.012	1.898	−1.106	58.27
30	0.900	0.872	0.058	−0.016	1.107	−0.833	75.24
40	0.928	0.900	0.077	−0.021	0.956	−0.775	81.06
50	0.941	0.910	0.100	−0.023	0.897	−0.710	79.15
60	0.950	0.962	0.106	−0.028	0.766	−0.665	86.81
70	0.970	0.968	0.124	−0.032	0.731	−0.627	85.65

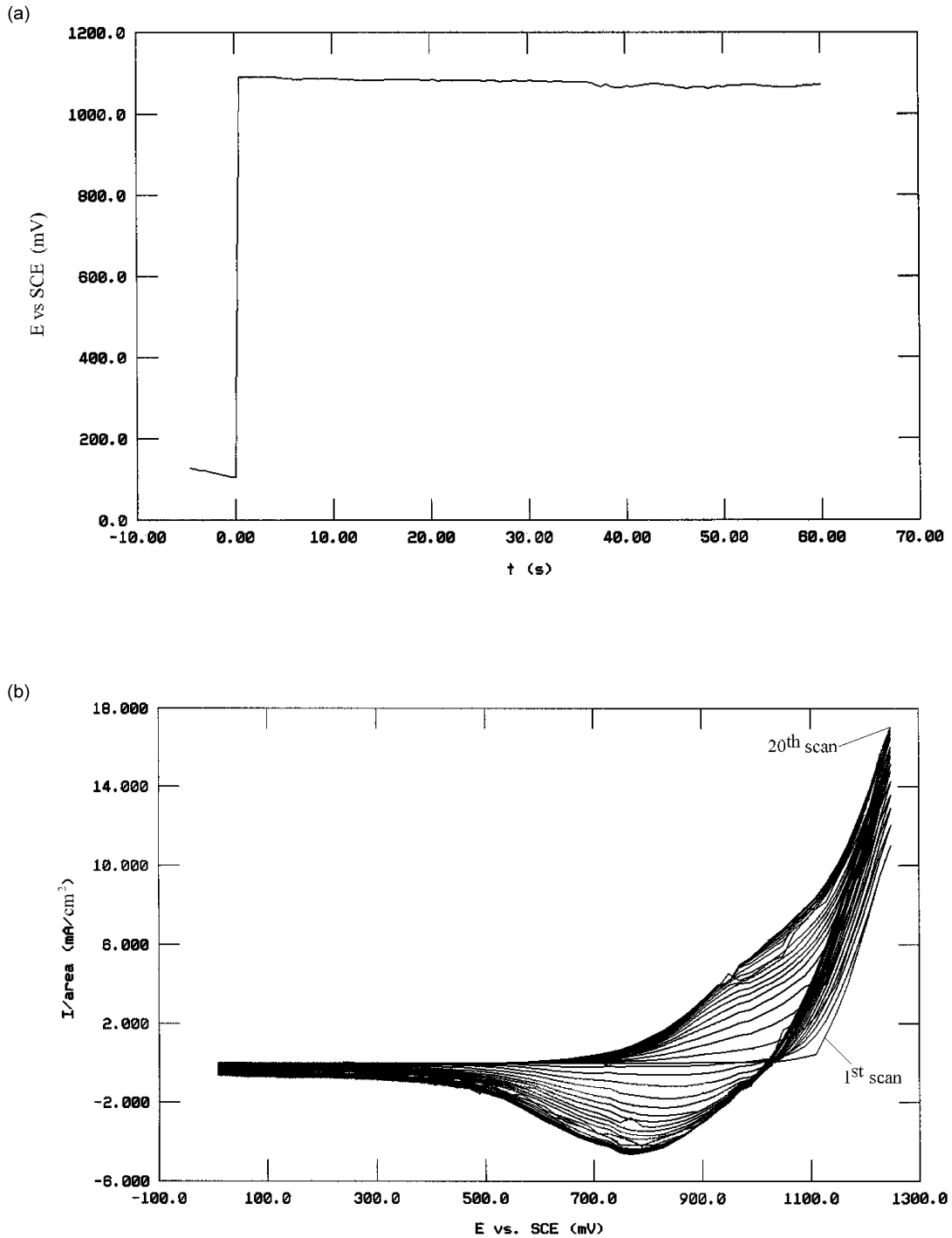

Fig. 2. (a) Electrochemical polymerization of biselenophene using 0.05 M in tetra-*n*-butylammonium-tetrafluoroborate electrolyte in acetonitrile at 25 °C, with a fixed current density of 0.5 mA cm^{-2}. (b) Electrochemical polymerization of biselenophene using cyclic voltammetry method, where biselenophene (0.05 M) was dissolved in (0.1 M) tetra-*n*-butylammonium-tetrafluoroborate electrolyte in acetonitrile at a scan rate of 50 mV s^{-1} on ITO glass for consecutive 20 scans.

energy absorption edge of the spectrum using the expression provided below [16]. In the expression, α is the absorption coefficient near the absorption edge, E_g is the band gap of the polymer. By plotting $(\alpha h\nu)^2$ versus $h\nu$ for the PBSE film in the band edge region, followed by extrapolation of the plot to zero, a direct band gap of 1.90 V is obtained. Upon comparisons of neutral dedoped polyselenophene films with PBSE, the band gap energy of PBSE (1.90 eV) is slightly lower than that of polyselenophene (2.0 eV). [15]

$$(\alpha h\nu)^2 = (\text{const})(h\nu - E_g)$$

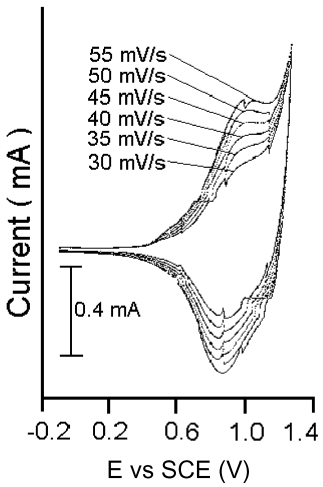

Fig. 3. Cyclic voltammetry of polybiselenophene using 0.1 M tetra-*n*-buthylammonium fluoroborate in dry acetonitrile conducted at different scan rates. PBSE was precoated on platinum foil (0.5 cm^2) using galvanostatic method from 0.05 M monomer solution.

3.5. In situ UV–Vis near infrared electrochemical doping studies

Fig. 4(a) shows the optical absorption spectra changes of PBSE taken in situ using UV–Vis near infrared during electrochemical doping. In the neutral state, PBSE showed a single absorption peak at 2.5 eV, which corresponded to the $\pi \rightarrow \pi^*$ interband transition and the polymer appeared reddish-brown in colour. When a potential of +0.9 V was applied, the peak height of the interband transition was suppressed and one new absorption peak appeared simultaneously at about 1.4 eV. While at higher oxidation potential, the peak height of interband transition was further suppressed and two absorption bands or polaron bands at 1.4 and 0.8 eV were observed. The heavily doped film was greenish blue in colour. These remarkable changes were typical characteristics of conducting polymers. Accordingly, these spectral changes may be interpreted in terms of the removal of electron from the valence band and the formation of p-type polaron bands upon electrochemical doping. The corresponding energy band diagram for PBSE can be represented accordingly as shown in Fig. 4(b). In the electrochemically doped state, two polaron states were observed inside the band gap at 0.8 eV above the valence band and 0.5 eV below the conduction band.

3.6. FTIR of monomer and polymers

The FTIR spectrum of biselenophene showed α-CH and β-CH out of plane bend at 689 and 788 cm^{-1}, C–H deformation in-plane bands at 1021, 1075, 1205 cm^{-1}, aromatic ring stretches at 1307, 1430, 1500, and 1645 cm^{-1} and C–H stretches at 3099 and 3115 cm^{-1}, respectively.

In the dedoped polybiselenophene (PBSE 1), the intensity of the α-CH out of plane bend was reduced

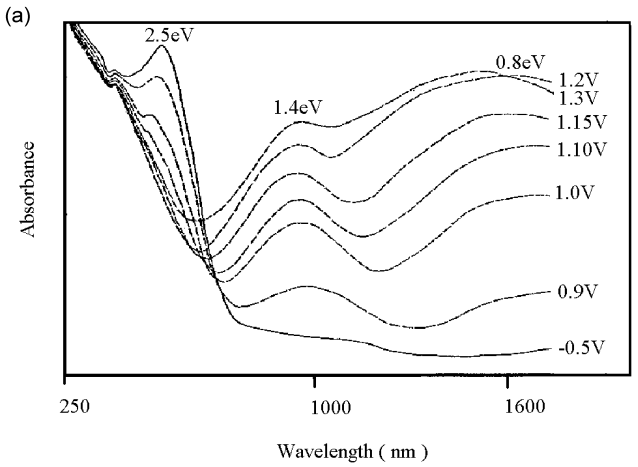

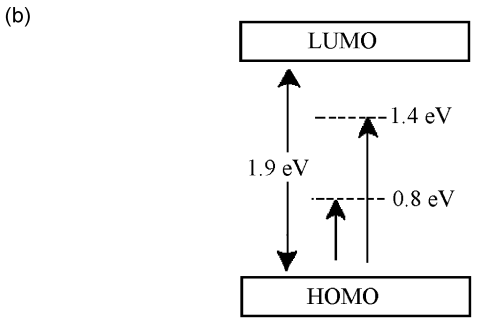

Fig. 4. (a) UV–Vis near infrared absorption spectral change of polybiselenophene taken in situ during electrochemical p-doping with (0.1 M) tetra-*n*-butyl ammonium BF_4^- doping in acetonitrile as a function of different applied potentials varying from −0.5 to +1.3 V versus SCE. (b) Energy band diagram for PBSE.

compared to the β-CH out of plane bend at 787 cm^{-1}, suggestive of predominant α–α′ coupling and some α–β coupling in the bulk polymer. Other C–H in-plane bends at 1020, 1070 cm^{-1} and ring stretches at 1437, 1498, 1560, 1658, and 1780 cm^{-1} were observed, indicating that the selenophene ring remained intact after polymerization. The iodine doped polybiselenophene (PBSE 3), showed significant broadening of peaks at region between 1020 and 1780 cm^{-1}. This region was characterized as the doping induced bands (1020, 1085, 1301, and 1410 cm^{-1}). The ferric chloride doped polybiselenophene (PBSE 2), showed a similar spectra as PBSE 3, with extensive masking of most of the fine peaks due to doping effects of the polymer.

3.7. Macroscopic DC conductivity of doped polymers

The conductivity measurements of both iodine and ferric chloride doped polymers were measured on pressed pellets using a conductivity meter. For iodine doped polymer, we have observed that with gradual increase in doping time, the polymer showed a gradual increase in iodine uptake with

simultaneous increase in conductivity reading until a saturation point at which the polymer showed no appreciable changes. The maximum conductivity reading obtained for iodine doped polybiselenophene, PBSE 3 was 0.1 S cm^{-1}. The iodine doped polybiselenophene was found to afford slightly higher conductivity than ferric chloride doped polybiselenophene, PBSE 2 (8×10^{-4} S cm^{-1}).

4. Conclusion

A novel electrically conducting polybiselenophene was successfully synthesized by both chemical and electrochemical methods. Optical studies of polybiselenophene on ITO glass showed bathochromic shift of its λ_{max} value with respect to polyselenophene from 440 to 498 nm. The optically derived band gap energy for polybiselenophene (1.9 eV) was also lower than that of polyselenophene (2.0 eV). Through electrochemical polymerization, a good electroactive polymer film having stable electrochemical p-doping process was obtained. Therefore in summary, through chemical modification of polymer backbone structure, the resulting optical and electrochemical properties of the polymer can be varied.

References

[1] Berlin A, Zotti G, Zecchin S, Schiavon G, Cocchi M, Virgili D, Sabatini C. J Mater Chem 2003;13:27.
[2] Gelenis S, Benz M, Legoff E, Schindler JL, Kanewurf CR, Kanatzidis MG. J Am Chem Soc 1993;115:12519.
[3] Ferraris JP, Bravo A, Kim W, Hrncis DC. J Chem Soc, Chem Commun 1994;991.
[4] Hillman AR, Mallen EF. J Electroanal Chem 1990;281:109.
[5] Hasoon S, Galtier M, Sauvajol JL. Synth Met 1989;28:C317.
[6] Salzner U, Lagowski JB, Pickup PG, Poirier RA. Synth Met 1998;96:177–89.
[7] Bezoari MD, Kovacic P, Gronowitz S, Hörnfeldt AB. J Polym Sci, Polym Lett Ed 1981;19:347–53.
[8] Bourahla A, Saiter JM, Vautier C. Mater Chem Phys 2001;69:163.
[9] Aqad E, Lakshikantham MV, Cava MP. Org Lett 2001;3:4283.
[10] Iwatsuki S, Kamei N, Kubo M. Chem Soc Jpn Chem Lett 1992;1551–4.
[11] Gronowitz S, Johnson I, Hornfeldt AB. Chem Scr 1975;7:111.
[12] Briscoe HVA, Peel JB. J Chem Soc 1928;1741.
[13] Wu G, Hozumi T, Kobei S, Naoya O. J Polym Sci, Polym Lett Ed 1981;19:397.
[14] Gronowitz S, Hornfeldt AB, Shabana R, Galal A, Mark HB, Zimmer H. Phosphorus Sulfur Silicon 1990;48:239.
[15] Spyridon G, David SG, Arthur JF. J Appl Phys 1987;62:190.
[16] Johnson EG. In: Willardson R, Beer AC, editors. Semiconductors and semimetals, vol. 3. New York: Academic; 1967. p. 153.
[17] Chan HSO, Ng SC. Prog Polym Sci 1998;23:1167.
[18] Zhang DH, Qin JG, Xue G. Synth Met 1999;106:161.
[19] Waltman FJ, Bargon J, Diaz AF. J Phys Chem 1983;87:1459.
[20] Tourillon G, Garnier F. J Electroanal Chem 1982;135:173.